Stars and their variability observed from space
C. Neiner, W. W. Weiss, D. Baade, R. E. Griffin, C. C. Lovekin, A. F. J. Moffat (eds)

SEARCH FOR QUIET STELLAR-MASS BLACK HOLES BY ASTEROSEISMOLOGY FROM SPACE

H. Shibahashi[1] and S. J. Murphy[2]

Abstract.
It is thought that stars with an initial mass more than $\sim 25\,\mathrm{M}_\odot$ ultimately become black holes. Stellar-mass black holes should therefore be ubiquitous, but fewer than 20 have been found in our Galaxy to date, and all of them have been found through their X-ray emission. In most cases these are soft X-ray transients – low-mass X-ray binaries whose optical counterparts are late-type stars filling their Roche lobes, giving rise to accretion onto black holes. In one case the stellar-mass black hole is in a high-mass X-ray binary whose optical counterpart is an early-type star. Its strong stellar winds are accreted by the black hole, producing X-ray emission. It follows that X-ray-quiet stellar-mass black holes exist in wide binary systems. The discovery of black holes in the optical region through their gravitational interactions would be a major scientific breakthrough. Recent space-based photometry has made it possible to measure phase or frequency modulations of pulsating stars to extremely high precision. Such modulations are caused by orbital motion, and analyses offer a lower limit for the mass of the companion to the pulsating star. If the companions are non-luminous and if their masses exceed the mass limit for neutron stars ($\sim 3\,\mathrm{M}_\odot$), they should be black holes. We review the methodology, and demonstrate analyses of some encouraging cases.

Keywords: Asteroseismology, Binaries: general, Stars: black holes, oscillations

1 Introduction

It is thought that stars with an initial mass more than $\sim 25\,\mathrm{M}_\odot$ ultimately become black holes. Though the mass thresholds are dependent on the metallicity of the stars and are currently uncertain, stars with an initial mass in the range ~ 25–$40\,\mathrm{M}_\odot$ are expected to form black holes following a supernova explosion. Even more massive stars collapse to black holes without a spectacular explosion (Heger et al. 2003). These events are thought to correspond to the observed phenomena known as “failed supernovæ”, in which sudden brightening occurs – as in the early stage of a supernova – but does not develop to full supernova luminosity (Adams et al. 2017). Stellar-mass black holes should therefore be ubiquitous. Population statistics of these stellar-mass black holes in our Galaxy may be estimated with a reasonable initial mass function, star formation rate, and assumptions of the density structure of the Galaxy. The uncertainty is large, but it is estimated that more than 100 million black holes reside in our Galaxy (Brown & Bethe 1994; Mashian & Loeb 2017; Breivik et al. 2017; Lamberts et al. 2018; Yalinewich et al. 2018; Yamaguchi et al. 2018).

Clearly there is no way to observe black holes directly. However, if a black hole is in a close binary system with an ordinary star, its presence can manifest itself in X-ray emission. If the black hole swallows gas from the companion star, a huge amount of potential energy is liberated, ultimately emitting X-rays that are detectable from space. However, X-ray binaries are not limited to systems containing a black hole. In general, they are close binaries composed of a compact object (a neutron star or a black hole) which is accreting mass from a companion donor star. Spectroscopic radial-velocity (RV) measurements of the optically visible donor enable us to deduce the lower limit of the invisible compact object, even if the latter is not itself visible. According to current theory, a neutron star more massive than $3\,\mathrm{M}_\odot$ is unstable and will collapse into a black hole. Therefore, a mass function that corresponds to a companion exceeding this critical mass is considered to be reliable evidence of a black hole. This is how stellar-mass black holes have been detected and confirmed (e.g., Cowley 1992; Remillard & McClintock 2006; Casares & Jonker 2014). Yet despite those estimates of 10^8 black holes in our Galaxy, fewer than 20 have so far been confirmed (Corral-Santana et al. 2016; Torres et al. 2019). If X-ray emission resulting from accretion only occurs in close binaries, quiescent stellar-mass black holes that show no X-ray emission would be limited to widely separated binaries.

[1] Department of Astronomy, School of Science, University of Tokyo, Tokyo 113-0033, Japan
[2] Sydney Institute for Astronomy, School of Physics, University of Sydney, NSW 2006, Australia

© Stars from Space

2 Black-hole X-ray binaries

About one third of X-ray binaries are not steadily visible but are detected as transient sources. Except for Cyg X-1, the Galactic stellar-mass black holes have so far been detected as transient X-ray sources in binaries with low-mass K- or M-dwarf companions (Tanaka & Shibazaki 1996). Figure 1 shows the γ-ray light-curve, obtained by the (*Swift* satellite) (Gehrels et al. 2004; Barthelmy et al. 2005), of such a low-mass X-ray binary, a *Ginga* source (GS 2023+338). Though their light-curves are individually different, these systems are often called X-ray novæ because of their X-ray brightening. The outbursts are caused by mass transfer instabilities in an accretion disc, which is fed by a low-mass dwarf (Mineshige & Wheeler 1989). During the γ-ray (and X-ray) outburst in 2015, the optical counterpart (known as V404 Cyg) brightened by ~ 6 mag in V. Such optical outbursts, labelled Nova Cygni 1938 by A. A. Wachmann, seem to be caused by reprocessing of X-ray photons in the accretion disk. In some other X-ray transients, the sudden optical brightening has also been classified as a nova (like Nova Vel 1993 in the case of GRS 100 9−45). The naming is misleading, since a classical nova is caused by a thermonuclear flash triggered by the accumulation of accreted gas on the surface of a white dwarf.

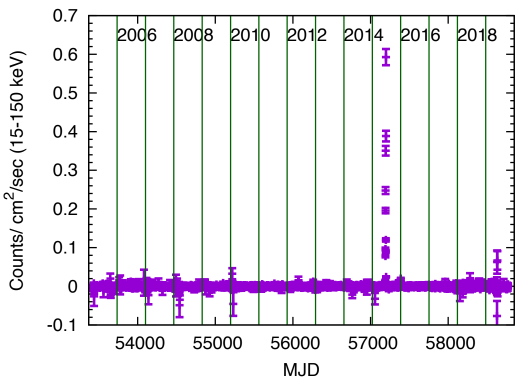

Fig. 1. γ-ray light-curve of GS 2023+338 obtained by *Swift*. Data were taken from the Swift archives.

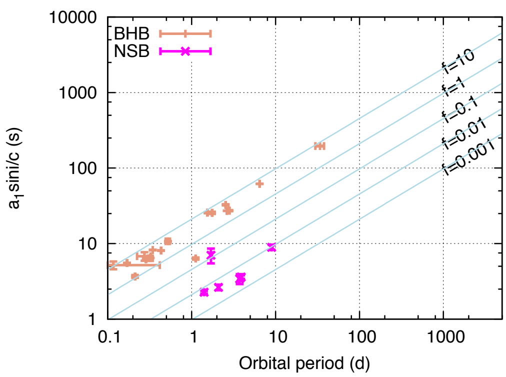

Fig. 2. Orbital period vs projected semi-major axis of X-ray binary systems.

In the X-ray quiescent phase between outbursts of GS 2023+338, V404 Cyg is as faint as $V \sim 18$ mag, and the optical source is the low-mass donor star itself (Casares et al. 2019); RV measurements therefore become possible and the orbital elements are deduced from them. The mass function giving the lower limit of the invisible compact object is determined from the orbital period $P_{\rm orb}$, the amplitude of RV variation $K_{\rm opt}$, and the eccentricity e:

$$f(M_{\rm opt}, M_{\rm X}, \sin i) \quad := \quad \frac{M_{\rm X}^3 \sin^3 i}{(M_{\rm opt}+M_{\rm X})^2} = \frac{1}{2\pi G} P_{\rm orb} K_{\rm opt}^3 \left(1-e^2\right)^{3/2}, \tag{2.1}$$

where $M_{\rm X}$ and $M_{\rm opt}$ denote the masses of the X-ray emitting, but optically invisible, compact object and of the optical counterpart, respectively, i is the inclination angle of the orbit, and G is the gravitational constant.

For V404 Cyg, the orbital period is 6.5 d and the amplitude of (almost sinusoidal) RV variations is $\sim 200\,{\rm km\,s^{-1}}$, so the mass function is $\sim 6\,{\rm M}_\odot$, giving a companion mass $M_{\rm X}$ much larger than the critical mass for a neutron star. This binary system therefore contains a stellar-mass black hole (Casares et al. 1992).

Besides GS 2023+338, 16 X-ray binaries have been confirmed, via spectroscopic RVs of the optical counterparts, to be composed of a late-type low mass star and a stellar-mass black hole. In addition, the presence of a stellar-mass black hole has been confirmed in Cyg X-1, whose optical counterpart is an early-type star (Webster & Murdin 1972; Bolton 1972). Its strong stellar winds are accreted by the black hole, producing X-ray emission. The binary properties of all of these Galactic black holes given in the literature are listed in Table 1 (Corral-Santana et al. 2016 and references therein). For each X-ray binary system, the projected semi-major axis of the optical counterpart, in units of light-seconds, is plotted versus the orbital period in Fig. 2, where both axes use a logarithmic scale. Here, the semi-major axis is

$$\frac{a_{\rm opt} \sin i}{c} = \frac{1}{2\pi c} P_{\rm orb} K_{\rm opt} \left(1-e^2\right)^{1/2}, \tag{2.2}$$

Table 1. Binary properties of the dynamically confirmed black-hole X-ray binaries in our Galaxy.

X-ray source	Opt.	Sp. Type	$P_{\rm orb}$ (h)	$f(M)$ ($\mathrm{M}_\odot$)	$M_{\rm BH}$ ($\mathrm{M}_\odot$)
Cyg X-1	HDE226868	O9Iab	134.4	0.244 ± 0.006	14.8 ± 1.0
GROJ0422+32	N. Per	M4-5V	5.09	1.19 ± 0.02	2 – 15
3A0620−003	N. Mon	K2-7V	7.75	2.79 ± 0.04	6.6 ± 0.3
GRS1009−45	N. Vel 93	K7-M0V	6.84	3.2 ± 0.1	> 4.4
XTEJ1118+480		K7-M1V	4.08	6.27 ± 0.04	6.9 – 8.2
GRS1124−684	N. Mus 91	K3-5V	10.38	3.02 ± 0.06	3.8 – 7.5
GS1354−64	BW Cir	G5III	61.07	5.7 ± 0.3	> 7.6
4U1543−475	IL Lup	A2V	26.79	0.25 ± 0.01	8.4 – 10.4
XTEJ1550−564		K2-4IV	37.01	7.7 ± 0.4	7.8 – 15.6
XTEJ1650−500		K4V	7.69	2.7 ± 0.6	< 7.3
GROJ1655−40	N. Sco 94	F6IV	62.92	2.73 ± 0.09	6.0 ± 0.4
1HJ1659−487	GX 339-4	> GIV	42.14	5.8 ± 0.5	> 6
H1705−250	N. Oph 77	K3-M0V	12.51	4.9 ± 0.1	4.9 – 7.9
SAXJ1819.3−2525	V4641 Sgr	B9III	67.62	2.7 ± 0.1	6.4 ± 0.6
XTEJ1859+226	V406 Vul	K5V	6.58	4.5 ± 0.6	> 5.42
GRS1915+105		K1-5III	812	7.0 ± 0.2	12 ± 2
GS2000+251	QZ Vul	K3-7V	8.26	5.0 ± 0.1	5.5 – 8.8
GS2023+338	V404 Cyg	K3III	155.31	6.08 ± 0.06	$9.0^{+0.2}_{-0.6}$

where c is the speed of the light. Systems of the same mass function would form a line with an inclination of 2/3. In the same diagram, some representative data for neutron-star X-ray binaries are plotted. As expected, most of the black-hole binaries (BHB) have a mass function larger than $1\,\mathrm{M}_\odot$, while the neutron-star binaries (NSB) have substantially smaller values.

Since the low-mass star is tidally locked, the spin period is the same as the orbital period. Hence the rotation velocity and the orbital velocity differ only by the factor of the ratio of the size of the star and the size of the orbit. The star fills its Roche lobe, so the size of the star is the Roche lobe size. The Roche lobe size relative to the binary separation is determined by the mass ratio (Paczyński 1971). Hence, the ratio of the rotation velocity to the orbital velocity gives the mass ratio. With a reasonable estimate for the mass of the low-mass star from its spectrum, the mass of the invisible object is thus observationally determined. The results taken from the literature are illustrated in Fig. 3 (Corral-Santana et al. 2016 and references therein). The X-ray objects with estimated masses in the range of 1.5–$3\,\mathrm{M}_\odot$ are neutron stars. X-ray transient systems containing an invisible object having a mass higher than $3\,\mathrm{M}_\odot$ are considered to be the best signatures of stellar-mass black holes.

X-ray binaries containing black holes are mostly distinguishable from those with neutron stars by their X-ray spectra. The former are characterised by an ultrasoft thermal component ($\lesssim 1.2$ keV), accompanied by a hard tail and seen after the flux reaches to the maximum, while the latter show a slightly harder ($\sim$ a few

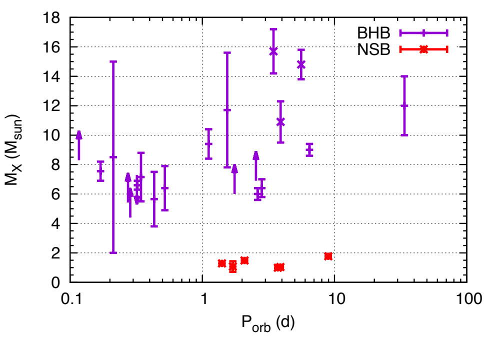

Fig. 3. Mass of the invisible compact object vs orbital period of X-ray binary systems.

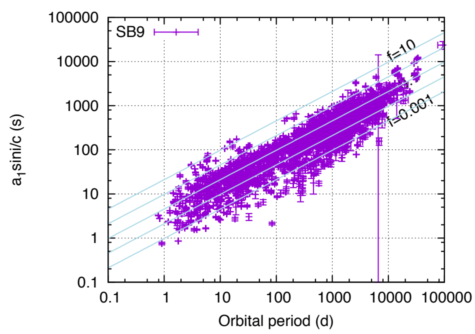

Fig. 4. Orbital period vs projected semi-major axis of binary systems listed in the *Ninth Catalogue of Spectroscopic Binary Systems* (SB9) (Pourbaix et al. 2004). Mass functions are shown in units of $\mathrm{M}_\odot$.

keV) black-body component, which is thought to be from the neutron star envelope, and a softer but still a bit harder component than the black-hole X-ray binaries, most probably from the accretion disk. Ultrasoft X-ray transient sources are regarded as a signature of binaries containing a black hole. There are ~ 60 such X-ray sources suspected to be black hole binaries from their spectra, and classified as "black-hole candidates", but not yet dynamically confirmed, so less secure (Corral-Santana et al. 2016 and references therein).

3 Search for quiet black holes in single-lined spectroscopic binaries

Quiescent black holes in wide binary systems may be found in RV surveys by searching for single-lined systems with high mass functions. Such an attempt was proposed by Guseinov & Zel'dovich (1966), who selected 7 plausible candidates in an attempt to detect "collapsed stars". Their attempt was later followed by Trimble & Thorne (1969) (see also Trimble & Thorne 2018) using the sixth catalogue of the orbital elements of spectroscopic binary systems (Batten 1967). For each system the mass of the primary star was estimated from its spectral type, and an approximate lower limit to the mass of the unseen companion was then calculated from the observed mass function. Trimble & Thorne (1969) listed 50 systems that had an unseen secondary star more massive than the Chandrasekhar mass limit for a white dwarf.

Figure 4 shows the distribution of spectroscopic binaries listed in SB9 (Pourbaix et al. 2004) in the plane of orbital period versus semi-major axis. More than 50 systems are found to have a mass function larger than $1\,\mathrm{M}_\odot$. However, in most cases careful follow-up observations unveiled the presence of a fainter secondary star of larger mass (e.g. Stickland 1997). A plausible scenario is that the primary was originally more massive than the secondary and it had evolved faster than the secondary. A substantial amount of mass loss in the red-giant phase made the primary significantly less massive than the secondary, which is still in the main-sequence phase and relatively much fainter than the evolved primary. Generally, a larger and more homogeneous sample of main-sequence stars is favourable; however, such a sample has been difficult to procure in practice. Spectroscopic data have to be collected as time-series covering the orbital phase of each binary system, often obtained one by one from ground-based observing sites with a large amount of observing time, and often with large telescopes for fainter stars. This forms a bottle-neck to such binary studies.

Since this conference, Thompson et al. (2019) found a black hole–giant star binary (2MASS J05215658+4359220), from multi-epoch RVs acquired by the APOGEE survey (Majewski et al. 2017). The system has a nearly circular orbit with $P_\mathrm{orb} = 83.2 \pm 0.06\,\mathrm{d}$, a semi-amplitude $K_\mathrm{opt} \simeq 44.6 \pm 0.1\,\mathrm{km\,s^{-1}}$ and a mass function of $0.766 \pm 0.006\,\mathrm{M}_\odot$. The photometric data vary periodically in step with the RV variations, implying spin-orbit synchronisation of the star. A combination of the measured projected spin velocity and the period leads to $R_\mathrm{opt} \sin i \simeq 23 \pm 1\,\mathrm{R}_\odot$; the mass of the giant star is estimated to be $M_\mathrm{opt} \sin^2 i \simeq 4.4^{+2.2}_{-1.5}\,\mathrm{M}_\odot$ from this radius and the spectroscopically estimated $\log g$. An independent combination of the apparent luminosity, the spectroscopically determined effective temperature and *Gaia* distance measurements gives $R_\mathrm{opt} = 30^{+9}_{-6}\,\mathrm{R}_\odot$, which is consistent with the value based on the spin velocity. As a consequence, from the aforementioned mass function, the minimum mass of the unseen companion is estimated to be $\sim 2.9\,\mathrm{M}_\odot$, marginally exceeding the critical mass for a neutron star. This is likely to be the first success at finding an X-ray quiet black hole lurking in a binary system, though within the uncertainties the companion could be a neutron star instead.

4 Search for quiet black holes based on phase modulations of pulsating stars in binaries

From *MOST* (Walker et al. 2003) to *CoRoT* (Auvergne et al. 2009), *Kepler* (Koch et al. 2010), *TESS* (Ricker et al. 2015) and *BRITE*-Constellation (Weiss et al. 2014), space-based photometry with extremely high precision over long time-spans has led to a drastic change of this situation, and has revolutionized our view of variability of stars. Some variability has been detected in almost all stars, and thousands of pulsating stars plus hundreds of eclipsing binaries (Kirk et al. 2016) have been newly discovered. *Kepler*'s 4-year simultaneous monitoring of nearly 200,000 stars also opened a new window onto a statistical study of binaries (Murphy et al. 2018; Murphy 2018; Shibahashi & Murphy 2019). This pedigree will be augmented further by *PLATO**.

Binary orbital motion causes a periodic variation in the path length of light travelling to us from a star, so if the star is pulsating, the time delay manifests itself as a periodically varying phase-shift in the form of the product with an intrinsic angular frequency (Shibahashi & Kurtz 2012; Shibahashi et al. 2015). The light arrival-time delay can then be measured by dividing the observed phase variation by the frequency (Murphy et al. 2014). The light-time effect upon the observed times of maxima in luminosity, which vary over the orbit,

*http://sci.esa.int/plato/59252-plato-definition-study-report-red-book/

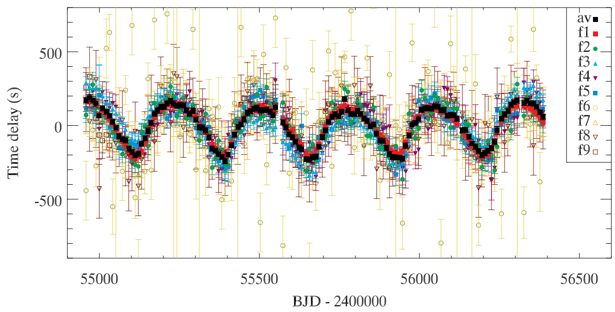

Fig. 5. An example of a time-delay curve (KIC 9651065) using 9 different pulsation modes. The weighted average is shown as filled black squares. Adopted from Murphy & Shibahashi (2015).

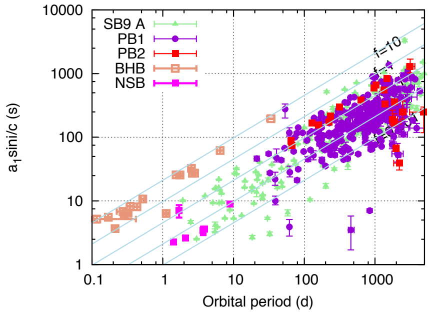

Fig. 6. Orbital period vs projected semi-major axis of newly discovered δ Sct binary systems, together with binaries having an A-type primary (as catalogued in SB9). Mass functions are shown in units of $M_{\odot}$.

has been used to find unseen binary companions (the so-called *O-C* method; e.g. Sterken 2005 and papers cited therein). Such a method works well in the case of stars pulsating with a single mode, since the intensity maxima are easy to track and any deviations from precise periodicity are fairly easy to detect. However, if the pulsating star is multiperiodic (as in the case of most objects observed from space), the situation is much more complex, and it is more suitable measure the time delay by careful analysis of phase modulation. Figure 5 shows a time-delay curve calculated with *Kepler* data. It immediately provides us with qualitative information about the orbit (Murphy & Shibahashi 2015; Murphy et al. 2016).

Murphy et al. (2018) applied this technique to all targets in the original *Kepler* field with effective temperatures ranging from 6600–10000 K, and discovered 341 new binary systems containing δ Scuti stars (main-sequence A stars pulsating in pressure modes). Importantly, many of those binaries would not have been detectable by other techniques, because A stars are often rapid rotators (Royer et al. 2007), making spectroscopic RVs difficult to measure. Using space-based photometry to measure the phase modulation of pulsating stars is a very efficient way of creating a homogeneous sample of binary systems. Indeed, these asteroseismically detected binaries tripled the number of intermediate-mass binaries with full orbital solutions, and, importantly, provided a homogeneous dataset for statistical analyses.

The newly detected binaries are plotted in the ($P_{\rm orb}$-$a_1 \sin i/c$)-diagram shown as Fig. 6, and (for comparison) the black-hole X-ray binaries listed in Table 1 and 162 spectroscopic binaries listed in the SB9 (2004) Catalogue having primary stars of similar spectral type (A0–F5). Only systems with full orbital solutions plus uncertainties were selected. The following should be noted: Binaries with orbital periods shorter than 20 d were not found by the asteroseismic method. This is because the light-curve is divided into short segments, such as 10 d, in order to measure the phases of pulsation modes of close frequencies. It is then unfavourable to deal with binary stars with orbital periods shorter than the segment size dividing the observational time span, which is typically $\sim$10 d. With short-period binaries also having smaller orbits (hence smaller light travel times), the binaries with periods in the range of 20–100 d are difficult to detect by the asteroseismic method and the sample in this period range must be considerably incomplete. It is also in this period range that binaries are most likely to exhibit eclipses, but eclipsing binaries were removed from the asteroseismic sample so as to avoid biasing the detection (Murphy et al. 2018).

The mass range of δ Scuti type stars used by Murphy et al. (2018) is $1.8 \pm 0.3\,M_{\odot}$. Those systems having a mass function larger than $\sim 1\,M_{\odot}$ are therefore thought to have a binary counterpart more massive than the neutron-star mass threshold, $\sim 3\,M_{\odot}$ and they may be regarded as systems containing a stellar-mass black hole. As shown in Fig. 6, several systems with large mass functions have been found. Those with a mass function larger than $1\,M_{\odot}$ are listed in Table 2. However, the seemingly massive secondary could itself be double or multiple, rendering each component less massive and fainter than expected. Indeed, some systems with large mass functions were eventually found to be triples, via follow-ups with ground-based RV observations made by Lehman, Murphy and their many collaborators (in preparation). In some other cases of highly eccentric orbits, the RV observations clarified the suspicion that the amplitude of phase modulation was simply overestimated (see Fig. 7). Nevertheless, there still remain a few systems that are found to be single-lined spectroscopic binaries with large mass functions. They could be systems with a massive white dwarf or a neutron star. Further detailed observations are required before conclusions can be considered definite.

Table 2. Binary properties of δ Sct stars in the *Kepler* field having a mass function larger than $1\,\mathrm{M}_\odot$.

KIC	P_{orb} (d)	$a_1 \sin i/c$ (s)	e	ϖ_1 (rad)	$f(M)$ ($\mathrm{M}_\odot$)
5219533	$1571.0^{+15.0}_{-13.0}$	$1367.0^{+11.0}_{-10.0}$	$0.5767^{+0.0081}_{-0.0081}$	$0.478^{+0.016}_{-0.013}$	$1.111^{+0.032}_{-0.032}$
8459354	$53.559^{+0.020}_{-0.022}$	$276.0^{+57.0}_{-76.0}$	$0.9809^{+0.0062}_{-0.0180}$	$6.085^{+0.034}_{-0.078}$	$7.9^{+4.9}_{-6.5}$

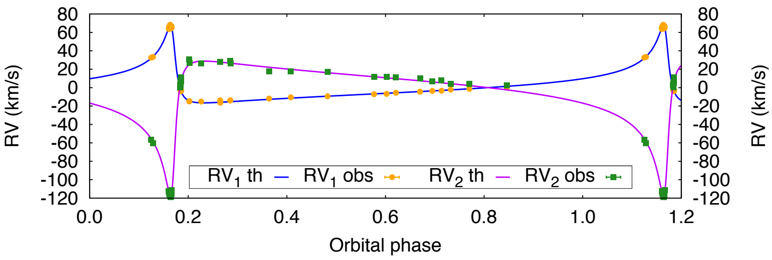

Fig. 7. An example of systems with highly eccentric orbits for which the RV observations confirmed that the amplitude of phase modulation was simply overestimated.

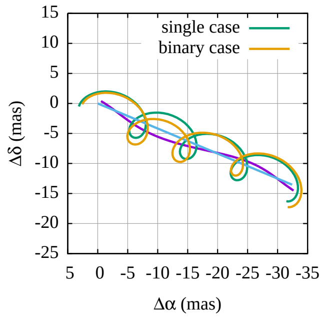

Fig. 8. Projected motion of a single star, and of a star in a binary system with an unseen companion.

5 Self-lensing black-hole binaries

In the case of an edge-on black-hole binary system (whose orbital axis is almost perpendicular to the line-of-sight), evidence for a lurking black hole would be available in addition to its large mass function. At superior conjunction, when the black hole transits in front of the optical companion, contrary to the case of an ordinary eclipsing binary, a luminosity brightening is induced by the gravitational microlensing (Einstein 1936; Leibovitz & Hube 1971; Maeder 1973). In the general case, the characteristic size of this lens (called the Einstein radius, R_{E}) is given by

$$R_{\mathrm{E}} := \sqrt{\frac{4GM_{\mathrm{BH}}}{c^2}\frac{d_{\mathrm{S}}}{d_{\mathrm{L}}}(d_{\mathrm{S}} - d_{\mathrm{L}})} \tag{5.1}$$

with the notation described in Gould (2000), where G is the gravitational constant, M_{BH} is the mass of the black hole, and d_{S} and d_{L} denote the distances to the source and to the lens, respectively. For the present case, $d_{\mathrm{S}} = d_{\mathrm{L}} + a(1-e^2)/(1 - e \sin \varpi_{\mathrm{opt}})$, where $a := a_{\mathrm{opt}} + a_{\mathrm{BH}}$ is the summation of the semi-major axes of the two components and ϖ_{opt} is the argument of the periapsis of the optical companion. Hence the Einstein radius, in units of light-seconds, is

$$\frac{R_{\mathrm{E}}}{c} = 4.44 \times 10^{-2} \left(\frac{a/c}{100\,\mathrm{s}}\right)^{1/2} \left(\frac{M_{\mathrm{BH}}}{\mathrm{M}_\odot}\right)^{1/2} \left(\frac{1-e^2}{1 - e\sin\varpi_{\mathrm{opt}}}\right)^{1/2} \mathrm{s}. \tag{5.2}$$

This is only a few percent of one solar radius, so the geometry for the lensing is narrowly restricted to the edge-on case; the inclination angle, i, should be in the range $\pi/2 - (R_{\mathrm{opt}}/a) \le i \le \pi/2 + (R_{\mathrm{opt}}/a)$.

The tangential velocity of the black hole relative to the optical component at the superior conjunction is

$$\frac{v_{\mathrm{t}}}{c} = \frac{2\pi(a/c)}{P_{\mathrm{orb}}}\frac{(1 - e\sin\varpi_{\mathrm{opt}})}{\sqrt{1-e^2}}. \tag{5.3}$$

The duration of the transit is then given by

$$\begin{aligned} t_{\mathrm{trans}} &:= \frac{2\sqrt{R_{\mathrm{opt}}^2 - a^2\cos^2 i}}{v_{\mathrm{t}}} \\ &= \frac{P_{\mathrm{orb}}}{\pi}\left\{\left(\frac{R_{\mathrm{opt}}}{a}\right)^2 - \cos^2 i\right\}^{1/2} \frac{\sqrt{1-e^2}}{1 - e\sin\varpi_{\mathrm{opt}}}. \end{aligned} \tag{5.4}$$

Luminosity brightening repeats at every superior conjunction, i.e., once per orbital period. Similar self-lensing systems containing white dwarfs have so far been found for five cases (Kruse & Agol 2014; Kawahara et al. 2018;

Masuda et al. 2019), so the probability to detect such a rare but physically important event is not necessarily hopeless (Masuda & Hotokezaka 2019).

The brightness enhancement of the microlens during the transit is $A(R_{\rm E}/R_{\rm opt})^2$, where we estimate A to be 1.27 by integrating light emitted from points behind the Einstein radius using equation 5 of Paczyński (1986). Therefore, the luminosity enhancement during the black-hole transit is of the order of a few percent in the case of $R_{\rm E}/R_{\rm opt} = 1/10$. The transit light curves (magnification versus time) of microlensing events resemble inverted planetary transits.

6 Search for quiet black holes by astrometry

Another promising method for finding quiet black-hole binaries uses *Gaia* astrometry, which is extremely sensitive to non-linear proper motions of astrometric binaries with periods in the range 0.03–30 years. Targets are not restricted to pulsating stars. *Gaia* is expected to detect "approximately 60% of the estimated 10 million binaries down to 20 mag closer than 250 pc"[†]. Like a simulation illustrated in Fig. 8, the orbital motion in each astrometric binary system can be seen directly, leading to the orbital elements and the mass functions. *Gaia* simultaneously carries out spectroscopic observations, though not for all stars. If the target has spectroscopy, the mass of the star can be estimated independently once its temperature is determined spectroscopically. If one component is unseen, its mass is deduced from the mass function and the spectroscopic mass of the optical counterpart. The unseen single companion should be either a white dwarf, a neutron star or a black hole, depending on its mass.

7 Sumary

(a) X-ray quiet BHBs are expected to be present. (b) Searching for X-ray quiet BHBs is challenging, but worth pursuing. (c) Space-based asteroseismology and the measurements of light arrival-time delays opened a new window on binary statistics. (d) Binary systems with unseen companions and high mass functions could result from the secondary being a black hole. (e) Self-lensing BHBs are expected to show periodic brightening. (f) Space-based astrometry also opens another window on binary statistics.

8 Acknowledgements

The authors thank the organizing committee of the conference, led by Werner Weiss, for their excellent organization, resulting in a fruitful meeting. This work was partly supported by the JSPS Grant-in-Aid for Scientific Research (16K05288).

References

Adams, S. M., Kochanek, C. S., Gerke, J. R., & Stanek, K. Z. 2017, MNRAS, 469, 1445

Auvergne, M., Bodin, P., Boisnard, L., et al. 2009, A&A, 506, 411

Barthelmy, S. D., Barbier, L. M., Cummings, J. R., et al. 2005, Space Sci. Rev., 120, 143

Batten, A. H. 1967, Publications of the DAO Victoria, 13, 119

Bolton, C. T. 1972, Nature Physical Science, 240, 124

Breivik, K., Chatterjee, S., & Larson, S. L. 2017, ApJ, 850, L13

Brown, G. E. & Bethe, H. A. 1994, ApJ, 423, 659

Casares, J., Charles, P. A., & Naylor, T. 1992, Nature, 355, 614

Casares, J. & Jonker, P. G. 2014, Space Sci. Rev., 183, 223

Casares, J., Muñoz-Darias, T., Mata Sánchez, D., et al. 2019, MNRAS, 488, 1356

Corral-Santana, J. M., Casares, J., Muñoz-Darias, T., et al. 2016, A&A, 587, A61

Cowley, A. P. 1992, ARA&A, 30, 287

Einstein, A. 1936, Science, 84, 506

Gehrels, N., Chincarini, G., Giommi, P., et al. 2004, ApJ, 611, 1005

Gould, A. 2000, ApJ, 542, 785

Guseinov, O. K. & Zel'dovich, Y. B. 1966, Soviet Astronomy, 10, 251 (Astronomicheskii Zhurnal, 43, 313)

Heger, A., Fryer, C. L., Woosley, S. E., Langer, N., & Hartmann, D. H. 2003, ApJ, 591, 288

[†]https://sci.esa.int/web/gaia/-/31441-binary-stars

Kawahara, H., Masuda, K., MacLeod, M., et al. 2018, AJ, 155, 144
Kirk, B., Conroy, K., Prša, A., et al. 2016, AJ, 151, 68
Koch, D. G., Borucki, W. J., Basri, G., et al. 2010, ApJ, 713, L79
Kruse, E. & Agol, E. 2014, Science, 344, 275
Lamberts, A., Garrison-Kimmel, S., Hopkins, P. F., et al. 2018, MNRAS, 480, 2704
Leibovitz, C. & Hube, D. P. 1971, A&A, 15, 251
Maeder, A. 1973, A&A, 26, 215
Majewski, S. R., Schiavon, R. P., Frinchaboy, P. M., et al. 2017, AJ, 154, 94
Mashian, N. & Loeb, A. 2017, MNRAS, 470, 2611
Masuda, K. & Hotokezaka, K. 2019, ApJ, 883, 169
Masuda, K., Kawahara, H., Latham, D. W., et al. 2019, ApJ, 881, L3
Mineshige, S. & Wheeler, J. C. 1989, ApJ, 343, 241
Murphy, S. J. 2018, arXiv e-prints, arXiv:1811.12659
Murphy, S. J., Bedding, T. R., Shibahashi, H., Kurtz, D. W., & Kjeldsen, H. 2014, MNRAS, 441, 2515
Murphy, S. J., Moe, M., Kurtz, D. W., et al. 2018, MNRAS, 474, 4322
Murphy, S. J. & Shibahashi, H. 2015, MNRAS, 450, 4475
Murphy, S. J., Shibahashi, H., & Bedding, T. R. 2016, MNRAS, 461, 4215
Paczyński, B. 1971, ARA&A, 9, 183
Paczyński, B. 1986, ApJ, 304, 1
Pourbaix, D., Tokovinin, A. A., Batten, A. H., et al. 2004, A&A, 424, 727
Remillard, R. A. & McClintock, J. E. 2006, ARA&A, 44, 49
Ricker, G. R., Winn, J. N., Vanderspek, R., et al. 2015, JATIS, 1, 014003
Royer, F., Zorec, J., & Gómez, A. E. 2007, A&A, 463, 671
Shibahashi, H. & Kurtz, D. W. 2012, MNRAS, 422, 738
Shibahashi, H., Kurtz, D. W., & Murphy, S. J. 2015, MNRAS, 450, 3999
Shibahashi, H. & Murphy, S. J. 2019, arXiv e-prints, arXiv:1909.07595
Sterken, C. 2005, The Light-Time Effect in Astrophysics: Causes and cures of the O-C diagram, ASP Conf. Ser., 335
Stickland, D. J. 1997, The Observatory, 117, 37
Tanaka, Y. & Shibazaki, N. 1996, ARA&A, 34, 607
Thompson, T. A., Kochanek, C. S., Stanek, K. Z., et al. 2019, Science, 366, 637
Torres, M. A. P., Casares, J., Jiménez-Ibarra, F., et al. 2019, ApJ, 882, L21
Trimble, V. & Thorne, K. S. 2018, arXiv e-prints, arXiv:1811.04310
Trimble, V. L. & Thorne, K. S. 1969, ApJ, 156, 1013
Walker, G., Matthews, J., Kuschnig, R., et al. 2003, PASP, 115, 1023
Webster, B. L. & Murdin, P. 1972, Nature, 235, 37
Weiss, W. W., Rucinski, S. M., Moffat, A. F. J., et al. 2014, PASP, 126, 573
Yalinewich, A., Beniamini, P., Hotokezaka, K., & Zhu, W. 2018, MNRAS, 481, 930
Yamaguchi, M. S., Kawanaka, N., Bulik, T., & Piran, T. 2018, ApJ, 861, 21